

January 1995

CfA Preprint No. 4019
astro-ph/9502004

Spectra and Statistics of Cosmic String Perturbations on the Microwave Background: A Monte Carlo Approach

Andrea M. Gilbert¹ and Leandros Perivolaropoulos²

*Harvard-Smithsonian Center for Astrophysics
60 Garden St.
Cambridge, MA 02138, USA.*

Abstract

Using Monte Carlo simulations of perturbations induced by cosmic strings on the microwave background, we demonstrate the scale invariance of string fluctuation patterns. By comparing string-induced fluctuation patterns with gaussian random phase ones, we show that the non-gaussian signatures of the string patterns are detectable by tests based on the moments of the distributions only for angular scales smaller than a few arcminutes and for maps based on the gradient of temperature fluctuations. However, we find that tests of the gaussianity of the moments fail when we include a reasonable amount of instrumental noise in a pattern. Signal to noise ratios of 3.3 or greater completely suppress a string pattern's non-gaussian features even at the highest resolutions.

¹E-mail address: agilbert@cfa.harvard.edu

²E-mail address: lperivol@cc.uoi.gr

1 Introduction

The major progress made during the last decade in both cosmological observation and theory has made the search for understanding of the origin of cosmic structure one of the most exciting fields of scientific research.

Two classes of theoretical models explaining the origin of structure have emerged during the last decade and have survived with only minor adjustments through strong constraints imposed by detailed observational data. According to the first class of models, the primordial fluctuations that gave rise to structure in the universe were produced by quantum fluctuations of a scalar field during a period of exponential growth of the size of the universe. This period is known as *inflation* and was invented in order to causally explain the observed large scale isotropy and homogeneity of the universe. The primordial fluctuations produced during inflation may be shown to obey Gaussian statistics and to have a *scale invariant* spectrum. In this context scale invariance means that the amplitude of fluctuations at the time when they enter the causally connected horizon is fixed (*i.e.* independent of cosmic time).

According to the second class of theories, primordial fluctuations are provided by *seeds* of trapped energy density produced during a phase transition in the early universe. Such phase transitions are predicted by particle physics theories known as Grand Unified Theories (GUT's), which attempt to unify all known interactions under a single theory. The transition is predicted to occur at 10^{-35} seconds after the Big Bang, when the temperature of the universe is about $10^{16} GeV$.

The seeds of energy produced during the phase transition are called *topological defects* and are effectively localized regions where the symmetric high temperature phase of the universe has been trapped and its decay to the present low temperature vacuum manifold is prevented by topological considerations. According to their geometry, topological defects are classified into monopoles (stable pointlike defects), cosmic strings (stable linear defects), domain walls (planar defects), and textures (collapsing pointlike defects). Most theories for large scale structure formation based on monopoles and domain walls face severe conflicts with observations and are not favored [1]. On the other hand, theories based on cosmic strings and textures show several encouraging features when compared with observations and are among the main contenders proposed to explain the origin of structure in the universe.

In what follows, we focus on observational tests for theories based on cosmic strings.

The formation and evolution of strings is described in a review by Vilenkin [2]. It has been shown, using both analytical arguments [2] and numerical simulations [3] of string network evolution, that the network of strings approaches a configuration which looks the same at all times with respect to the causal horizon scale. This configuration is known as the *scaling solution*. According to this solution the string network at any given time consists of about 10 long strings

with radii of curvature of the order of the causal horizon scale, along with a component of small string loops with radii much smaller than the horizon scale [3].

The presence of such a network in the universe results in several observational predictions which can be used to test the underlying theory. The most important prediction is that of large scale structure formation. At early times, the cosmic string network produces density and velocity perturbations in the surrounding matter. These perturbations grow gravitationally and can lead to the presently observed structure in the universe. It has been shown [4, 5] that the mass per unit length (μ) of strings required in order to get bound structures by today is

$$G\mu \simeq 10^{-6} \quad (1)$$

where G is Newton's constant, included to obtain a dimensionless number. This condition is consistent with requirements imposed by microphysics in order to make GUT's consistent with particle physics accelerator experiments [6, 7]. If this condition is satisfied, the cosmic string model predicts the existence of the following: filaments and sheets of galaxies (formed in the wakes of moving long strings) with thicknesses comparable with observations [5, 8, 9, 10]; coherent large-scale velocity fields [11, 12]; perturbations on the microwave background sky [13]; and galactic magnetic fields [14]. It also predicts the existence of ultra-high energy gamma ray events [15, 16], gravitational lensing of quasars [17], and a stochastic gravitational radiation background [18]. Despite the large number of predictions made by the string model and the detailed existing data, it has not been possible to rule out the model using any particular observation. This is due in part to the complexity of the model, which introduces large uncertainties in its predictions, but it may also be due to features of the model which could contain elements of the physically realized theory.

The recent detection of fluctuations on the 2.7K microwave background sky, first by the COBE collaboration on angular scales of 10° [13] and later by other experiments on smaller angular scales, has provided a powerful new tool for testing theoretical models. The main source of string-induced fluctuations on the microwave background at large angular scales is the *Kaiser-Stebbins effect*.

According to the Kaiser-Stebbins effect, a moving long string present between the last scattering surface (the horizon at the time of recombination t_{rec}) and the present time t_0 produces temperature discontinuities between photons reaching the observer from opposite sides of the string (Figure 1). These discontinuities have the form of a step function [19, 20], and are caused by the geometry of spacetime around the string; the space around a straight long string is locally flat, but globally it has the geometry of a cone with a deficit angle equal to $8\pi G\mu$ [21]. Thus, a moving long string interacts nontrivially with microwave background photons.

The magnitude δT of these discontinuities is given by:

$$\frac{\delta T}{T} = \pm 4\pi G\mu v_s \gamma_s \hat{k} \cdot (\hat{v}_s \times \hat{s}), \quad (2)$$

where \vec{v}_s is the velocity of the string, \hat{k} is the unit wave vector of the perturbed photon, and \hat{s} is a unit vector along the string. Due to the effects of compensation [22, 23] and finite string radius of curvature, the scale over which these discontinuities persist is about equal to the radius of curvature of the long string, which according to the scaling solution is approximated by the causal horizon scale at the time when the photon interacted with the string. An observer scanning the sky along a line which intersects a long string will detect a temperature perturbation pattern which cuts off at horizon scales due to the above effects; the degree of sharpness of the cut-off is not well-determined, but Magueijo has shown that compensation is affected by a gravitational shock front, which implies a sharp cutoff of the gravitational effects of long strings at horizon scales [24]. We therefore approximate the temperature perturbation of a long string as a step function whose cut-off at the horizon scale is discontinuously sharp, and whose width is proportional to the horizon scale at the time when the string was present. It follows that the predicted temperature pattern along a line on the sky may be found by superposing the step functions corresponding to all strings present from t_{rec} to the present, t_0 . This model for the Kaiser-Stebbins effect has the most discontinuous possible cut-off, so if the actual form of the string seed function is less discontinuous, our results are too optimistic.

The construction of patterns of string-induced cosmic microwave background fluctuations suggests two interesting classes of tests for the string model. The first class involves the properties of the power spectrum $P(k)$ of the pattern of fluctuations $F(\theta) = \frac{\delta T}{T}(\theta)$, a function of the angle θ along an arc of a great circle in the sky. The Fourier transform of the pattern is given by

$$f(k) = \int_{-\infty}^{\infty} F(\theta) e^{-ik\theta} d\theta, \quad (3)$$

and the power spectrum $P(k)$ is then defined as the ensemble average of the squared magnitude of the Fourier transform,

$$P(k) = \langle |f(k)|^2 \rangle, \quad (4)$$

where $\langle \rangle$ denotes ensemble average.

The temperature fluctuations detected in the COBE experiment have been shown to have slightly different spectral indices n for different methods of calculating n , but these values are all consistent with a scale invariant spectrum. Bennett *et. al.* find $n \approx 1.4 \pm 0.5$ [25], and Wright *et. al.* find $n \approx 1.2 \pm 0.4$ using a basis other than the spherical harmonics in order to account for the omission of data in the region of the galactic plane [26]. Scale invariant perturbations are democratic perturbations for which no particular scale is favored over others, and whose amplitude is the same for both large and small scales. For scale invariant perturbations along an arc on the sky, it may be shown that [27] $kP(k) = \text{constant}$. The power spectrum is considered scale invariant when

its correlation function, the Fourier transform of the power spectrum, is constant for all θ . The correlation function smoothed on an angular scale θ_0 is given by

$$C(\theta)_{\theta_0} = \langle \frac{\delta T}{T}(\theta_1) \frac{\delta T}{T}(\theta_1 + \theta) \rangle_{\theta_1} \approx \frac{1}{2\pi} \int e^{ik\theta} P(k)W(k - k_0)dk, \quad (5)$$

where $k_0 \equiv \frac{\pi}{\theta_0}$ and $W(k - k_0)$ is a filter function filtering out smoothed modes. For scale invariant perturbations we have

$$C(0)_{\theta_0} \approx \int P(k)W(k - k_0)dk \approx \text{constant}, \quad (6)$$

where $\langle \rangle_{\theta_1}$ indicates an average over all θ_1 [28]. Therefore the *rms* temperature fluctuations corresponding to a scale invariant spectrum are independent of the smoothing scale.

Since string-induced temperature perturbations are produced by a superposition of step functions whose amplitude is constant on the average and whose scales vary continuously from a minimum scale equal to the horizon at t_{rec} to a maximum scale equal to the horizon at t_0 , we expect this model to produce a spectrum that is scale invariant for a wide range of scales. In the next section we will test this prediction using Monte Carlo simulations.

The second class of tests involves the identification of the non-gaussian features of string perturbations.

One of the main predictions of models based on inflation is that the probability distribution of primordial perturbations is described by a gaussian. Since the microwave background is a direct window to these primordial perturbations, inflation predicts that the probability $Q(\delta)$ for detecting a temperature fluctuation $\delta = \frac{\delta T}{T}$ in a given pixel along an arc of the sky in an experiment is given by

$$Q(\delta) = \frac{1}{\sqrt{2\pi\sigma^2}} \exp\left(-\frac{\delta^2}{2\sigma^2}\right), \quad (7)$$

where $\sigma = \left(\frac{\delta T}{T}\right)_{rms}$ is the root mean square temperature fluctuation obtained from all pixels.

On the other hand, cosmic string perturbations are produced by superposition of seed functions. Such a superposition in general leads to a non-gaussian probability distribution for the resulting perturbations. However, in the limit of a very large number of superposed seeds per pixel, the central limit theorem [29] predicts that the resulting perturbations will be gaussian to a good approximation. The number of superimposed seeds per pixel increases as the resolution of an experiment decreases. Thus for large angular scale experiments such as COBE, whose resolution is 10° , cosmic strings predict gaussian behavior of perturbations. The degree of non-gaussianity of string perturbations depends crucially on the parameters of the scaling solution. For a large number of strings per horizon volume, M , we expect the perturbations to remain gaussian down

to small angular scales. Numerical simulations of string network evolution indicate $M \approx 10$, which may be large enough to wipe out non-gaussian signatures on scales of one degree or even smaller.

In this work we use Monte-Carlo simulations to construct one-dimensional patterns of string-induced temperature fluctuations. We then use these patterns to test the scale invariance of the perturbations as well as quantify the dependence of the non-gaussian features on the resolution, the instrument noise, and the scaling solution parameters.

We describe in the next section the approximation used in the Monte Carlo simulations to construct the temperature fluctuation patterns for both the string and inflation theories. We approximate the fluctuations using step function superposition. The power spectrum of the resulting pattern is used to create a random phase realization pattern which is constructed by assigning random phases to the Fourier mode amplitudes obtained from the spectrum. Thus we have a gaussianized distribution for comparison with the initial one which has exactly the same power spectrum. Any differences between the two patterns are due not to spectrum differences but to the non-gaussian features of the stringy pattern. We use Fast Fourier Transform methods to obtain the power spectra of fluctuation patterns and thus show explicitly the range of scales over which the scale invariance persists. We justify our results via qualitative arguments.

In Section 3 we use the constructed temperature patterns to compare the probability distributions of fluctuations generated by cosmic strings and by inflation. We show explicitly that the non-gaussian features of the string patterns are only evident for microwave background experiments of very high resolution and find the minimum resolution required to distinguish the two models. We also show that this result is extremely sensitive to instrumental noise; even a modest amount of gaussian noise is enough to destroy all non-gaussian features on small scales.

Finally, in Section 4 we conclude and discuss interesting extensions of this project.

2 Simulations and Spectra

We construct patterns of cosmic microwave background fluctuations by dividing the time between recombination and the present into a set of discrete expansion time steps and applying string perturbations at each step. This type of multiple impulse approximation for strings was devised by Vachaspati [30] and first applied to microwave background fluctuations by Perivolaropoulos [31]. The earliest perturbation and first step occurs at the recombination time t_{rec} , when the angular size $\theta(t_{rec})$ of the causal horizon scale is about 2° . The angular size of the horizon grows with time according to

$$\theta(t) \approx \left(\frac{a(t)}{a(t_0)}\right)^{\frac{1}{2}} \approx t^{\frac{1}{3}}, \quad (8)$$

where $a(t)$ is the scale factor of the universe, and during the matter-dominated era when the string perturbations would have taken place, $a(t) \approx t^{\frac{2}{3}}$. Each subsequent step occurs when the causal horizon scale t doubles in size. Namely,

$$t_{i+1} = 2t_i \implies \theta_{i+1} = 2^{\frac{1}{3}}\theta_i, \quad (9)$$

where

$$\theta_1 = \theta(t_{rec}) \simeq 2^\circ. \quad (10)$$

Consider a lattice of N pixels along an arc of the sky with size Θ . At the i th time step,

$$t_i = 2^i t_{rec}, \quad (t_{rec} < t_i < t_0), \quad (11)$$

and our lattice includes q_i angular horizon scales, where

$$q_i = \frac{\Theta^\circ}{2^{i/3} 2^\circ}. \quad (12)$$

Let $M \simeq 10$ be the number of long strings per horizon in the scaling solution as predicted by numerical simulations of string networks [3]. Then the total number of randomly located step function perturbations n_i to be superposed on the pixel array during the i th expansion step is the product of the number of horizons and the number of strings per horizon,

$$n_i = M q_i = \frac{M \Theta^\circ}{2^{\frac{i}{3}} 2^\circ}. \quad (13)$$

The angular size ξ_i of each step function is approximately equal to the horizon size at the time step when the seed perturbs the lattice, so we have

$$\xi_i = 2^{\frac{(i-1)}{3}} 2^\circ. \quad (14)$$

Since we are not interested in the overall normalization of the fluctuation patterns, we choose the amplitude of each step function to be a random number in the range $[-1, 1]$. This accounts for the random velocities and orientations of long strings (see Eq. (2)). By performing the superposition of seeds as determined by the above quantities for each time step, we produce a pattern of seed fluctuations. When the angular size of the step functions and thus the horizon size becomes larger than the size of our lattice, the time steps end because such large seeds affect all of the pixels by the same amount and do not change $\frac{\delta T}{T}$, the fluctuation pattern.

After the pattern is constructed, we use FFT methods to find the Fourier transform of the completed pattern and thus its power spectrum as given in Eq. (4), by averaging over 100 realizations.

For each string fluctuation pattern, we also construct a corresponding ‘‘random phase realization’’ (RPR) of the pattern which serves as an approximation

to the type of pattern predicted by inflation theories. The RPR is the new temperature fluctuation pattern obtained by randomizing the phases of the Fourier modes and then using them to reconstruct a different pattern. This pattern is the best approximation we can make to inflationary fluctuations without changing the power spectrum of the pattern. Thus the RPR pattern $g(\theta)$ is given by

$$g(\theta) = \sum_{k=-\infty}^{+\infty} e^{(ik\theta)} |f(k)| e^{(i\theta_k)}, \quad (15)$$

where θ_k is a random number in the range $[-\pi, \pi]$. By the central limit theorem, the large number of terms in the sum (15) implies that the pattern $g(\theta)$ will be random, obeying a gaussian probability distribution.

First we demonstrate the scale invariant nature of the string-induced perturbations in patterns produced by our approximation. Figure 2 is a plot of $\log kP(k)$ versus $\log k$ for an experiment with resolution 2° (where $P(k)$ is the ensemble average of 100 realizations). For the slope we found

$$kP(k) \approx k^{-0.16 \pm 0.10}, \quad (16)$$

which is consistent with a scale invariant spectrum with $kP(k)$ approximately constant, and spectral index $n \approx 0.84 \pm 0.10$. As discussed in the introduction, we expected this result since the angular scale of the horizon at the recombination time was only 2° and the sizes of seeds spanned all larger scales; thus we see a scale invariant spectrum over a large range of scales. There are no seeds smaller than the minimum horizon size of 2° because any perturbations on photons produced before t_{rec} are erased by multiple scattering on the plasma. Thus scale invariance breaks down for scales less than 2° . Perivolaropoulos gives a simple analytic derivation of the scale invariance of the string fluctuations and the range of scales in which it should persist, *i.e.*

$$k \in \left[-\frac{\pi}{\theta_{min}}, \frac{\pi}{\theta_{min}} \right], \quad (17)$$

which depends on the angular scale of the last scattering horizon, $\theta_{min} \simeq 2^\circ$ [27].

We have demonstrated the scale invariance of the string-induced perturbations, a result that is consistent with COBE data, but which does not distinguish the predictions of the inflation model from those of the cosmic string model. This distinction may be made by examining the non-gaussian features of the fluctuations in the statistics of their distributions.

3 Non-Gaussian Features

As discussed in the introduction, most models based on inflation predict that the probability distribution of microwave background temperature fluctuations

is described by the gaussian of Eq. (7). The same kind of gaussian distribution, with different variance, is predicted for any linear combination of neighboring pixels, such as the temperature difference between two adjacent pixels. In what follows, we use this property of patterns of temperature differences to examine the non-gaussian features predicted for patterns of string-induced perturbations created by our Monte Carlo simulations.

Two mechanisms tend to suppress the non-gaussian character of a string fluctuation pattern. The first is the consequence of the central limit theorem, which states that a gaussian probability distribution results from the superposition of a large number of random variables which may have non-gaussian probability distributions. Thus the gaussian is an attractor for all other probability distributions. The distribution of string-induced fluctuations will therefore appear gaussian if the number of seeds perturbing each pixel is large; this occurs in low resolution experiments in which the angular size of each pixel is large, and in theories which predict a large number of seeds per horizon, *i.e.* $M = 10$ for strings.

The second mechanism is instrumental noise, which hides the non-gaussian signatures by superposing a gaussian distribution of noise upon them. The typical signal to noise ratio for microwave background experiments is about 2.

A useful way to determine whether a distribution in a random variable x obeys a gaussian probability distribution is to compare the moments of x with the corresponding moments of a gaussian. The n th moment λ_n of a distribution in x is defined as

$$\lambda_n = \frac{\langle x^n \rangle}{\langle x^2 \rangle^{\frac{n}{2}}} = \frac{\int x^n f(x) dx}{(\int x^2 f(x) dx)^{\frac{n}{2}}}, \quad (18)$$

where $f(x)$ is the probability distribution of the random variable x . The third and fourth moments are known as the skewness and kurtosis. For a gaussian distribution, the skewness is 0 and the kurtosis is 3. In practice, the skewness and kurtosis are obtained by using N measured values of the temperature fluctuation, where N would for example be the number of pixels in an experiment. Thus, even for a gaussian distribution the values $\lambda_3 = 0$ and $\lambda_4 = 3$ would not be obtained for finite N . Instead, the moments of a discrete distribution with finite but large N are random variables with gaussian probability distributions centered about the ideal values of the moments (*i.e.* those for which N approaches infinity), and with standard deviation σ which is proportional to $(\frac{1}{N})^{\frac{1}{2}}$ ($\sigma_{\lambda_3} = \sqrt{\frac{15}{N}}, \sigma_{\lambda_4} = \sqrt{\frac{96}{N}}$). Thus a temperature fluctuation pattern may be characterized as non-gaussian if the measured value of its kurtosis or skewness lies at least 1σ from the gaussian value.

The moments as defined in terms of the generating function of a distribution may be used to illustrate the effects of the central limit theorem on seed-induced fluctuation patterns. In general the generating function $M_\delta(t)$ is the Laplace

transform of the probability distribution $P(\delta)$ of the variable δ , defined by

$$M_\delta(t) = \int e^{t\delta} P(\delta) d\delta \implies \langle \delta^n \rangle = \frac{d^n}{dt^n} M(t) |_{t=0}, \quad (19)$$

where t is a dummy variable. Thus the n th derivative of the generating function of a variable is the n th moment of the distribution. The probability distribution of Eq. (7) may be rewritten through a change of variable as

$$P(\delta) = \frac{1}{\sqrt{2\pi}} e^{-\frac{\delta^2}{2}}. \quad (20)$$

Then the generating function of the gaussian is given by

$$M_\delta(t) = e^{\frac{t^2}{2}}, \quad (21)$$

and the definition (19) gives for the skewness $\lambda_3 = 0$ and for the kurtosis $\lambda_4 = 3$. An important property of generating functions is that for two variables δ_1 and δ_2 , their generating functions satisfy

$$M_{\delta_1+\delta_2} = M_{\delta_1} M_{\delta_2}. \quad (22)$$

The central limit theorem states that if

$$\delta_n = x_1 + \dots + x_n, \quad (23)$$

and

$$P(x_1) = \dots = P(x_n), \quad (24)$$

then as $n \rightarrow \infty$,

$$P(\delta_n) \rightarrow \frac{1}{\sqrt{2\pi\sigma_n^2}} e^{-\frac{\delta_n^2}{2\sigma_n^2}}. \quad (25)$$

The temperature fluctuation pattern for gaussian perturbations may be expanded in Fourier modes as

$$\delta = \frac{\delta T}{T}(\theta) = \sum_{k=-\infty}^{\infty} |\delta_k| e^{i\theta_k} e^{ik\theta}. \quad (26)$$

The gaussian probability distribution $P(\delta)$ is given in Eq. (20). For string-induced perturbations, the temperature fluctuation pattern is given by

$$\delta = \frac{\delta T}{T}(\theta) \approx \sum_{i=1}^n f_1^\psi(\theta - \theta_i), \quad (27)$$

where f_1 is a seed function (step-like) superposed at random angular locations θ_n . The generating function for the moments of the fluctuation due to the first seed x_1 is

$$M_{x_1}(t) = \langle e^{tx_1} \rangle = (pe^t + pe^{-t} + (1-2p)e^0), \quad (28)$$

where $p = \frac{\psi}{L}$ is the probability that the step function perturbation affects a given pixel. By the property of Eq. (22), we have for the generating function of moments of the combined fluctuations of many seeds

$$M_{\delta_n=x_1+\dots+x_n} = M_{x_1} * \dots * M_{x_n} = (2p \cosh(t) + (1 - 2p))^n. \quad (29)$$

In the limit $t \ll 1$, we can expand Eq. (29) to obtain

$$\left(1 + \frac{(2pn)t^2}{2n}\right)^n, \quad (30)$$

which for large number of seeds $n \gg 1$ approaches a gaussian limit,

$$M_{\delta_n} \longrightarrow e^{\frac{\sigma_n^2 t^2}{2}}. \quad (31)$$

From Eq. (28) function we can calculate the moments of the seed fluctuation pattern according to Eq. (19):

$$\lambda_2 = \sigma_n^2 = \frac{d^2}{dt^2} M_\delta(t) = 2np, \quad (32)$$

$$\lambda_3 = \frac{d^3}{dt^3} M_\delta(t) = 0, \quad (33)$$

$$\lambda_4 = \frac{d^4}{dt^4} M_\delta\left(\frac{t}{\sigma_n}\right) = 3 + \frac{1 - 6p}{2np} \longrightarrow 3. \quad (34)$$

Thus we have shown that in accordance with the central limit theorem, the moments of the string-induced fluctuation pattern approach the values of the corresponding moments of the gaussian probability distribution for large numbers of seeds.

We use the moments to compare our string-induced fluctuation patterns with their RPRs and thus find the values of parameters such as signal to noise ratio and experimental resolution which allow us to detect the non-gaussian nature of a string pattern. As described in Section 2, we create the patterns of string fluctuations from superposition of step function perturbations on a one-dimensional array of 512 pixels; the inflationary patterns follow by randomizing the phases of the Fourier modes of the string fluctuations (the RPR), but retaining the same power spectrum as that of the string pattern. We varied the values of angular resolution (or pixel size) and signal to noise ratio, and constructed 100 patterns for each case. The 100 patterns were used to calculate the means and standard deviations of λ_3 and λ_4 for each experiment.

Instrumental noise was introduced by adding to the temperature fluctuation value of each pixel an uncorrelated gaussian random component such that the ratio of the standard deviation of this component to the standard deviation of the true signal (temperature fluctuation) was set equal to the inverse of the signal to noise ratio $((s/n)^{-1})$. (Where the noise is zero we do not define s/n .)

Although measurements of microwave background radiation are plagued by correlated non-gaussian noise from our galaxy as well as instrumental noise, the effects of galactic noise are usually minimal compared to the latter because galactic noise can be modeled and subtracted from the data. In addition, even full sky maps such as those of COBE exclude data from the galactic plane. Residual galactic noise would have a small non-gaussian influence on the kurtosis of the fluctuations, but this effect would be the same at all experimental resolutions because galactic noise is continuous. The galactic non-gaussian component in the kurtosis of the temperature fluctuations thus remains constant with improving resolution, in contrast to the kurtosis of string-induced fluctuations which rapidly increases with increasing resolution because of the discontinuous nature of string seeds, as we will show. Thus the non-gaussian character of galactic noise would be easily distinguishable from that of string-induced fluctuations at high resolutions. Since adding galactic noise would only shift the kurtosis of a fluctuation pattern up by the same small amount at all resolutions, we neglect it, and include only uncorrelated gaussian noise in our model.

The step functions superposed to create the string fluctuations are antisymmetric, so it is equally likely for a temperature perturbation to be positive or negative. Thus the skewness predicted for the string pattern is zero, since this moment measures the symmetry of a distribution. Since zero is also the ideal value of the gaussian skewness, the skewness is not useful for distinguishing the string and gaussian patterns. We therefore focus on the statistics of the kurtosis λ_4 in what follows. (It has been shown that for higher moments of string patterns, the non-gaussian character is more easily detected than for the kurtosis, but the errors for higher moments increase faster than the degree of non-gaussianity, so we do not consider them [32].)

Figure 3 is a plot of kurtosis versus angular resolution with zero noise for both string and gaussian temperature fluctuation patterns. The values of λ_4 for both the seed and gaussian patterns are nearly the same, approximately the gaussian value of 3, for even the highest resolutions considered (0.5 arcmin). Thus even under the best experimental conditions (very high resolution and zero noise), this kurtosis test cannot distinguish between the two temperature fluctuation patterns. The number of seeds falling on the array is large enough to obscure the non-gaussian character of the seed perturbations as the central limit theorem predicts.

In order to improve our chances of observing the non-gaussian signatures of string perturbations, we cannot lower the number of seeds perturbing each horizon ($M = 10$) at each expansion step, since it is fixed by numerical simulations of the string scaling solution. We can, however, decrease the influence of the other factor causing large numbers of seeds to perturb a given pixel, the width of each seed step function; each step function affects all of the pixels within its horizon, and by the end of the simulation one perturbation spans the whole pixel array. The way to eliminate this effect is to examine the difference between temperature fluctuations in adjacent pixels, which is proportional to the derivative

of the pattern. In this case the seeds superposed are not step functions but delta functions localized at the discontinuities induced by the step functions. We thus dramatically decrease the number of perturbations which influence each pixel, improving our chance of observing any non-gaussian characteristics in the string patterns.

The success of this method in revealing the difference between the seed and gaussian fluctuations is demonstrated in Figure 4, in which we plot the kurtosis of the gradient of fluctuations versus resolution, and compare the patterns and their RPRs with zero noise. The plot shows that the non-gaussianity of the seed fluctuations is clear only for very good resolutions of less than 0.1° (6 arcminutes). The error bars indicate 1σ deviations; since the seed and gaussian errors do not overlap at high resolutions, we can distinguish fairly well between the two patterns for experiments with such resolution.

However, any realistic experiment will necessarily include some level of instrumental noise. Will the predicted non-gaussian features persist when the effects of noise are taken into account?

We addressed this question by adding a modest amount of noise ($s/n = 3.3$) to the temperature fluctuation maps and their RPRs and then constructing the temperature difference maps. In Figure 5, a plot of λ_4 versus angular resolution, we show that the noise completely removed the non-gaussian features for all resolutions. Though examining the temperature differences reduces the effect of too many seeds leading to gaussianity in the moments, it also greatly reduces the amount of “signal” in the average pixel, since it only counts the delta function spikes of the seed. The amplitude of the noise added depends on the standard deviation of the temperature fluctuation pattern from its mean, however, not the deviation of the temperature gradient pattern. It thus overwhelms the small amount of non-gaussian information in the gradient pattern and produces a pattern composed mainly of gaussian noise whose moments are highly gaussian.

We conclude that unless the amount of instrumental noise is unrealistically low ($s/n \simeq 10$ or greater), it is extremely difficult to detect the non-gaussian character of the cosmic string fluctuations using tests based on the skewness or kurtosis.

An obvious way to amplify the non-gaussian features predicted by models based on topological defects is to decrease the number M of superposed seeds per horizon scale. To do this we must consider models based on topological defects other than strings, since for strings M is fixed by simulations to be about 10. In the case of textures, for instance, we expect to find that tests based on the kurtosis will be more successful than they are with strings, because simulations predict that their value of M is about 0.05. While 10 strings appear in each horizon, only 1 texture forms and collapses in every 20 horizons at a given time. For non-string types of seeds, the structures of the perturbations they cause are not the same as the step function model appropriate for strings; the forms of the other seed perturbations are in general not discontinuous, so their probability distributions are more gaussian than that of the superposed step functions.

However, keeping in mind that we may be overestimating the non-gaussian features, we may use the step functions to obtain a rough answer to the following question: What is the maximum number of seeds M per horizon scale for a model in order for this model to have detectable non-gaussian features for resolutions of about 1 arcminute and $s/n \approx 5$?

In Figure 6, a plot of kurtosis λ_4 versus M for experiments with $s/n = 5$ and resolution of 1 arcminute shows that the maximum M for which the kurtosis is clearly not gaussian is 0.1. This suggests that it may be possible to detect non-gaussian signatures of the texture model for experiments with resolution $\theta_{min} \leq 1$ arcminute and $s/n \geq 5$.

4 Conclusion and Outlook

We have compared the temperature fluctuation and temperature gradient patterns created by Monte Carlo simulations based on a simple model for cosmic string fluctuations in the cosmic microwave background. We confirmed that our patterns have scale invariant power spectra over a wide range of scales, in agreement with COBE observations and the predictions of the topological defect and inflation theories; we showed that the kurtosis test can detect the non-gaussian features of the seed patterns, but for strings this test fails when we include even a small amount of instrumental noise because of the large number of seeds per horizon $M = 10$. For seed perturbations of the form of the string step function, the maximum value of M for which we might expect to detect the non-gaussian characteristics of a pattern is about 0.1, but this is an optimistic figure since other topological defects generally induce seed perturbations which are smoother than those of strings.

Since the moments are capable of distinguishing seed and gaussian patterns only in experiments with unrealistically low amounts of noise, they are not a viable test with which to analyze observed temperature fluctuation patterns and determine the nature of the primordial perturbations in the CMB. The study of other tests on the statistics of seed and gaussian patterns, such as the correlation of the Fourier phases of the power spectra, may produce more positive results.

5 Figure Captions

Figure 1: Kaiser-Stebbins Effect. A cosmic string with a velocity component perpendicular to the observer's line of sight induces a temperature perturbation $\frac{\delta T}{T}$ in microwave background photons crossing its path within a horizon scale.

Figure 2: This plot of $\log kP(k)$ versus $\log k$ shows the large range over which the fluctuation pattern is scale invariant. It has a nearly constant slope of -0.16 ± 0.10 , which gives the spectral index $n \approx 0.84 \pm 0.10$.

Figure 3: Plot of kurtosis of temperature fluctuations versus angular resolution (θ_{min}) with zero noise. Even at the highest resolutions, this test cannot distinguish the gaussian from the string pattern.

Figure 4: Plot of kurtosis of temperature gradient of fluctuations versus angular resolution. For high resolutions and zero noise, this test can distinguish between seed and gaussian patterns.

Figure 5: Same as Figure 4 but with gaussian instrumental noise added. A signal to noise ratio of 3.3 destroys all trace of the non-gaussian features of the seed pattern.

Figure 6: Plot of kurtosis versus number of seeds per horizon for seeds of the form of step functions. For the smallest values of M the kurtosis of string patterns deviates most from the gaussian, suggesting that fluctuation patterns for seeds with smaller M values such as textures would be more easily distinguished from the gaussian than string patterns.

References

- [1] R. Brandenberger. *Int. J. Mod. Phys.* **A9**, 2117 (1994) and references therein.
- [2] A. Vilenkin. *Phys. Rep.* **121** (1985).
- [3] D. Bennet and F. Bouchet. *Phys. Rev. Lett.* **D41**, 2048 (1990).
B. Allen and E.P.S. Shellard. *Phys. Rev. Lett.* **64**, 119 (1990).
D. Bennett and F. Bouchet. *Phys. Rev. Lett.* **60**, 257 (1988).
- [4] N. Turok and R. Brandenberger. *Phys. Rev.* **D33**, 2175 (1986).
- [5] L. Perivolaropoulos, R. Brandenberger, and A. Stebbins. *Phys. Rev.* **D41**, 1764 (1990).
- [6] P. Langacker. *Phys. Rep.* **22**, 185 (1981).
- [7] D. Perkins. *Am. Rev. Nucl. Part. Sci* **34**, 1 (1984).
- [8] T. Vachaspati. *Phys. Rev. Lett.* **57**, 1655 (1986).
- [9] A. Stebbins *et. al.* *Ap. J.* **322**, 1 (1987).
- [10] T. Vachaspati and A. Vilenken. *Phys. Rev. Lett.* **67**, 1057 (1991).
- [11] T. Vachaspati. *Phys. Lett.* **B282**, 305 (1992).
- [12] L. Perivolaropoulos and T. Vachaspati *Ap. J. Lett.* **423**, L77 (1993).
- [13] G. Smoot *et. al.* *Ap. J. Lett.* **396**, L1 (1992).
- [14] T. Vachaspati. *Phys. Rev.* **D45**, 3487 (1992).
- [15] J.H. MacGibbon and R. Brandenberger. *Phys. Rev.* **D47**, 2283 (1993).
- [16] R. Brandenberger, A. Sornborger, and M. Trodden. *Phys. Rev.* **D48**, 940 (1993).
- [17] D.N. Vollick and W.G. Unruh. *Phys. Rev.* **D44**, 2388 (1991).
- [18] R.R. Caldwell and B. Allen. *Phys. Rev.* **D45**, 3447 (1992).
- [19] N. Kaiser and A. Stebbins. *Nature* **310**, 391 (1984).
- [20] A. Stebbins. *Ap. J.* **327**, 584 (1988).
- [21] A. Vilenkin. *Phys. Rev.* **D23**, 852 (1981).
- [22] J. Traschen, N. Turok, and R. Brandenberger. *Phys. Rev.* **D34**, 919 (1986).
- [23] J.C.R. Magueijo. *Phys. Rev.* **D46**, 3360 (1992).

- [24] J.C.R. Magueijo. *Phys. Rev.* **D46**, 1368 (1992).
- [25] C.L. Bennett, *et. al.* *Ap. J.* **436**, 423 (1994).
- [26] E.L. Wright, *et. al.* *Ap. J.* **436**, 443 (1994).
- [27] L. Perivolaropoulos. *Spectral Analysis of Microwave Background Perturbations Induced by Cosmic Strings*, preprint submitted to *Ap. J.* (1994).
- [28] G. Efstathiou. In *Physics of the Early Universe*, SUSSP 36, 1989, ed. J. Peacock, A. Heavens, and A. Davies (IOP Publ., Bristol, 1990).
- [29] M. Spiegel *Probability and Statistics*, Editor: McGraw-Hill (1975).
- [30] T. Vachaspati. *Phys. Lett.* **B282**, 305 (1992).
- [31] L. Perivolaropoulos. *Phys. Lett.* **B298**, 305 (1992).
- [32] L. Perivolaropoulos. *Phys. Rev. D* **D48**, 1530 (1993).
R. Moessner, L. Perivolaropoulos, and R. Brandenberger. *Ap. J.* **425**, 365 (1994) (1993).

This figure "fig1-1.png" is available in "png" format from:

<http://arxiv.org/ps/astro-ph/9502004v2>

This figure "fig2-1.png" is available in "png" format from:

<http://arxiv.org/ps/astro-ph/9502004v2>

This figure "fig1-2.png" is available in "png" format from:

<http://arxiv.org/ps/astro-ph/9502004v2>

This figure "fig1-3.png" is available in "png" format from:

<http://arxiv.org/ps/astro-ph/9502004v2>

This figure "fig1-4.png" is available in "png" format from:

<http://arxiv.org/ps/astro-ph/9502004v2>

This figure "fig1-5.png" is available in "png" format from:

<http://arxiv.org/ps/astro-ph/9502004v2>

Log Power Spectrum

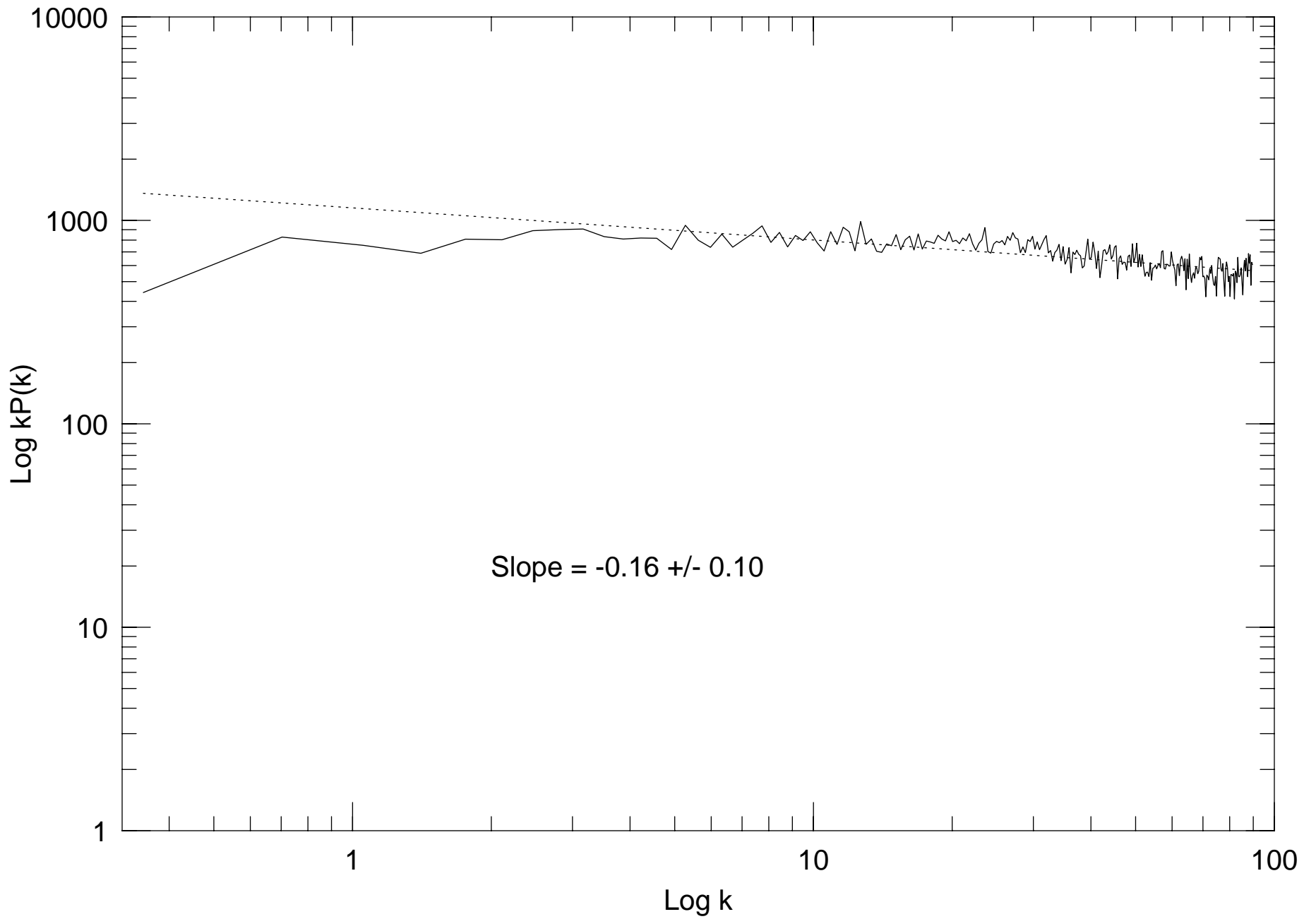


Figure 2

Kurtosis of $x = \delta T/T$

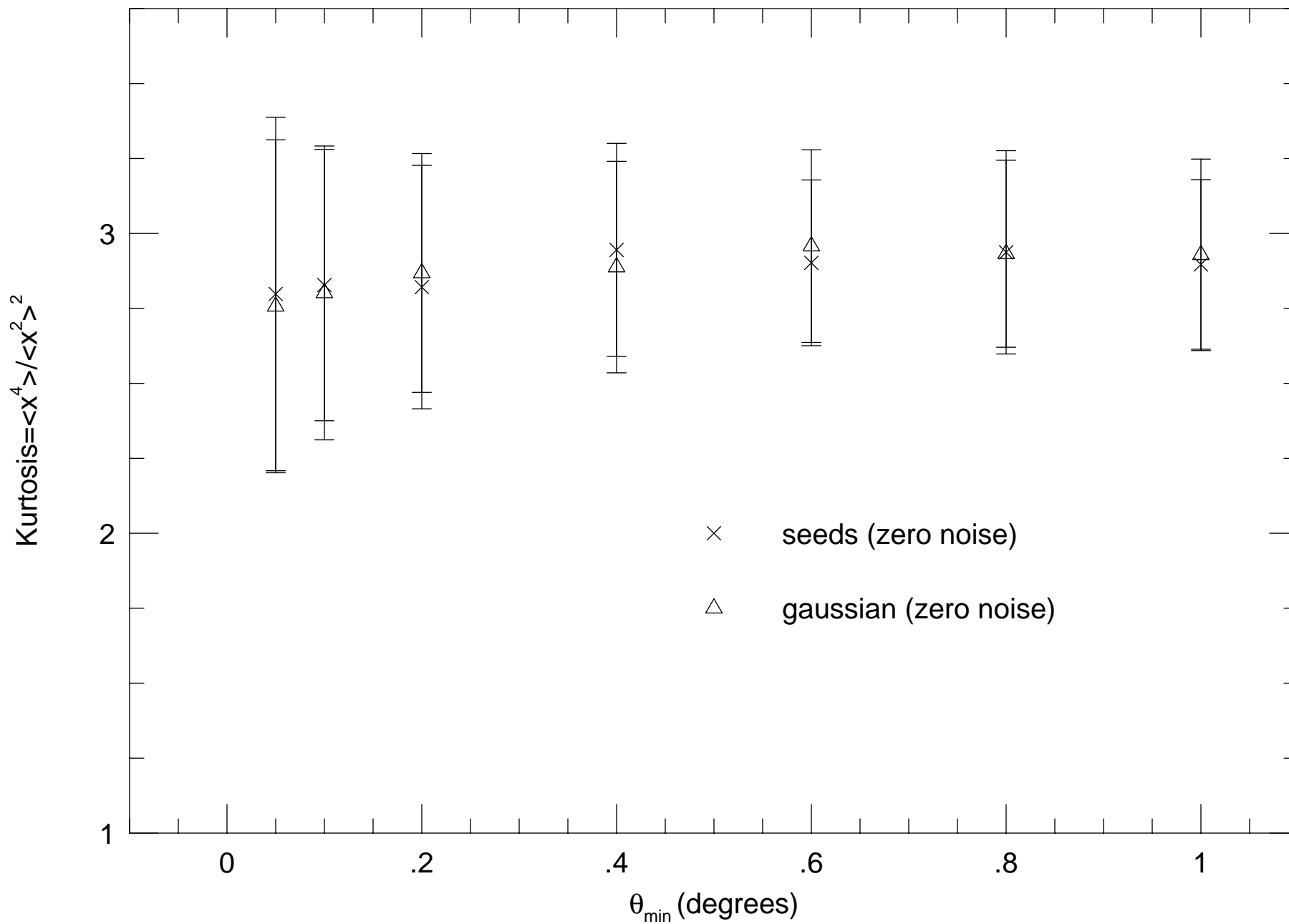


Figure 3

Kurtosis of $x=\text{Gradient of } \delta T/T$

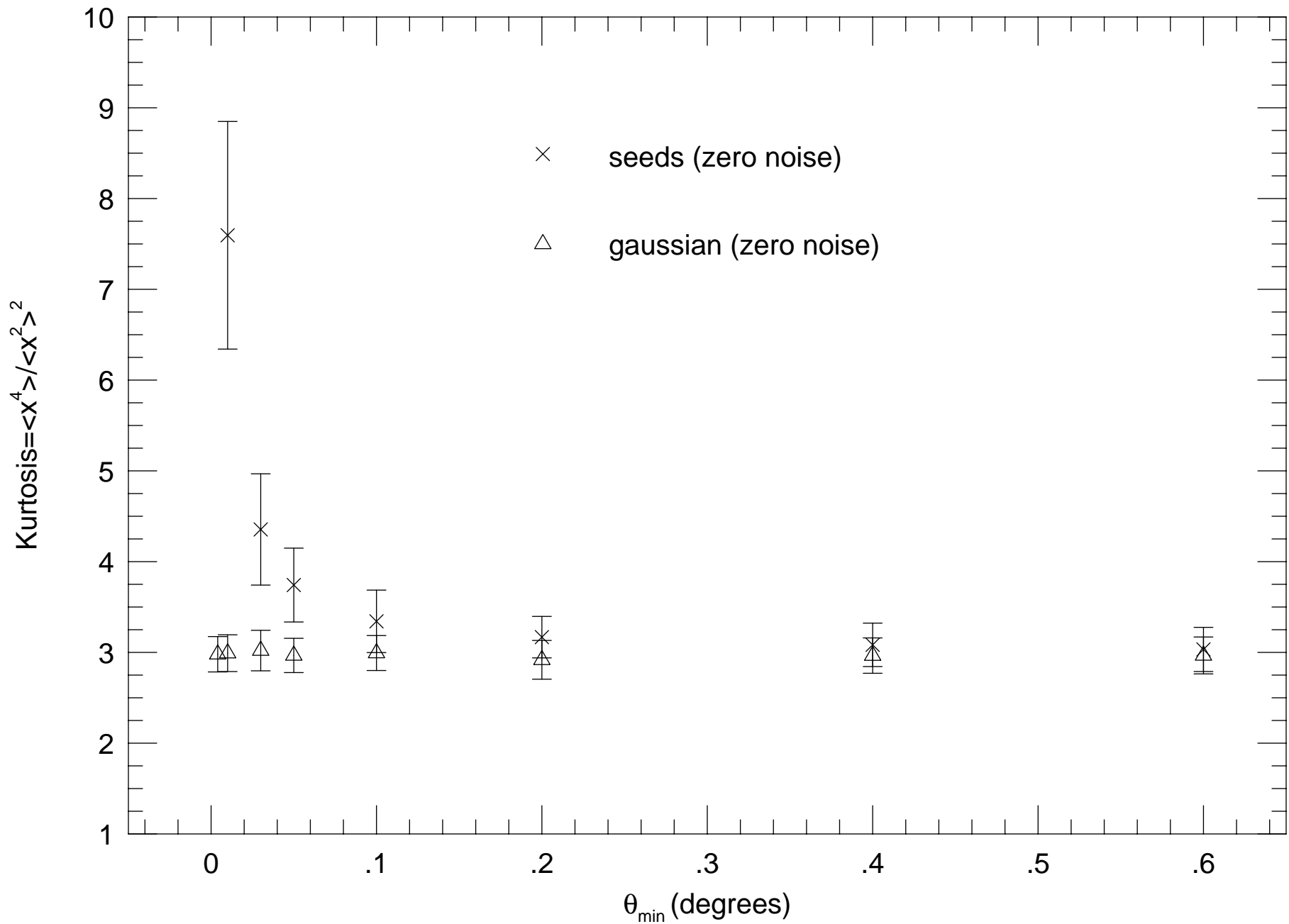


Figure 4

Kurtosis of $x = \text{Gradient of } \delta T/T$

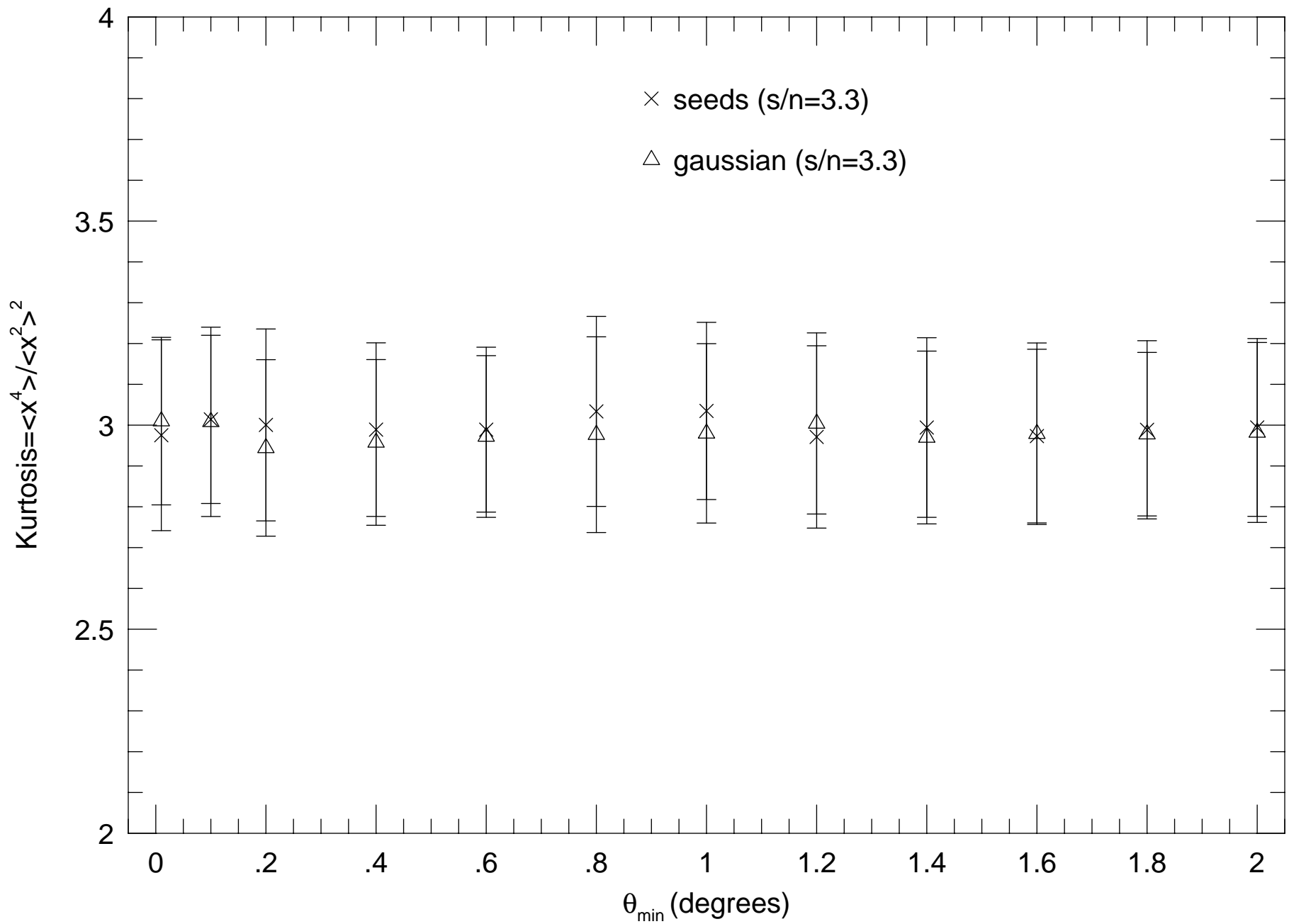


Figure 5

Kurtosis of x vs. M ($x = \text{Gradient of } \delta T/T$)

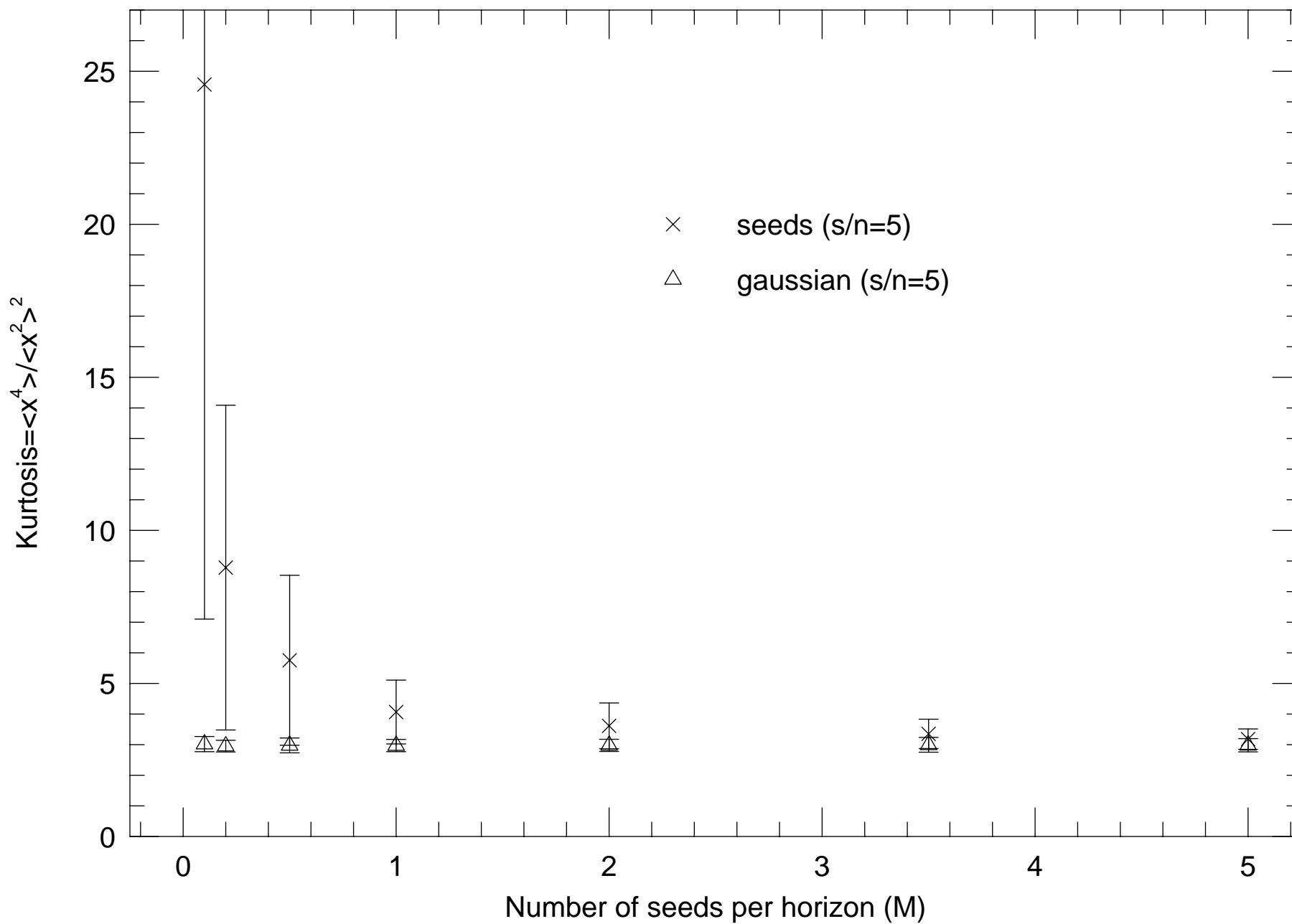


Figure 6

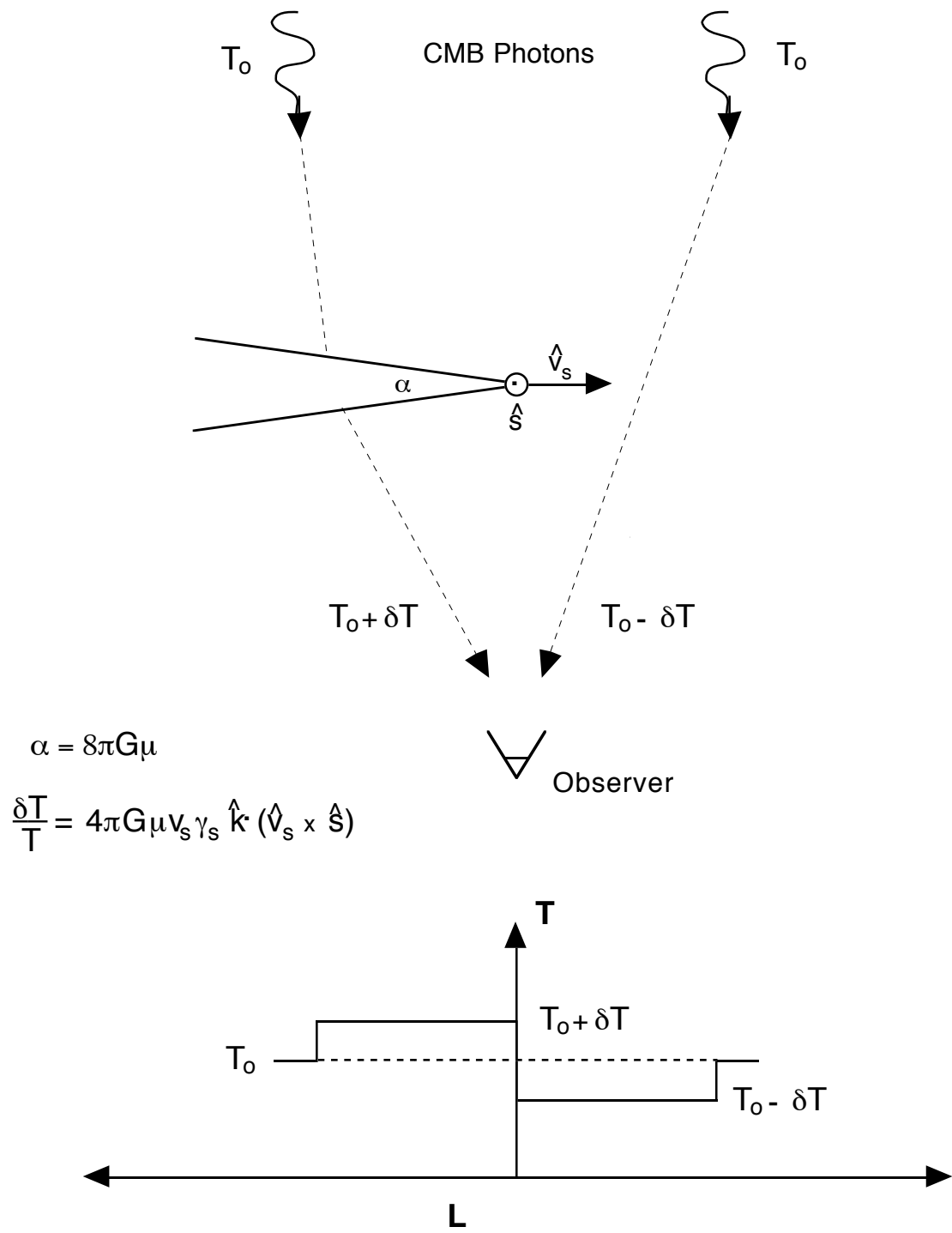


Figure 1